RSC Advances

PAPER

View Article Online
View Journal | View Issue

Cite this: *RSC Adv.*, 2023, **13**, 1558

GelMA/κ-carrageenan double-network hydrogels with superior mechanics and biocompatibility†

Xueqi Gan,‡[a] Chen Li,‡[a] Jiyu Sun,[a] Xidan Zhang,[a] Min Zhou,[a] Yi Deng *[acd] and Anqi Xiao*[b]

Hydrogels are crosslinked hydrophilic polymer networks of high-water content. Although they have been widely investigated, preparing hydrogels with excellent mechanical properties and biocompatibility remains a challenge. In the present work, we developed a novel GelMA/κ-carrageenan (GelMA/KC) double network (DN) hydrogel through a dual crosslinking strategy. The three-dimensional (3D) microstructure of KC is the first network, and covalently crosslinked on the κ-carrageenan backbone is the second network. The GelMA/KC hydrogel shows advantages in physical properties, including higher compression strength (10% GelMA/1% KC group, 130 kPa) and Young's modulus (10% GelMA/1% KC group, 300), suggesting its excellent elasticity and compressive capability. When using a higher concentration of GelMA, the hybrid hydrogel has even higher mechanical properties. In addition, the GelMA/KC hydrogel is favorable for cell spreading and proliferation, demonstrating its excellent biocompatibility. This study provides a new possibility for a biodegradable and high-strength hydrogel as a new generation material of orthopedic implants.

Received 27th September 2022
Accepted 17th December 2022

DOI: 10.1039/d2ra06101e

rsc.li/rsc-advances

1 Introduction

Hydrogels are insoluble hydrophilic polymers with a three-dimensional (3D) structure.[1,2] With the development of medical materials, natural polymer hydrogels have attracted considerable attention due to their unique properties, such as biocompatibility and biodegradability.[3] However, most have poor mechanical strength due to their physical structure and ample water content, limiting the application of natural polymer hydrogels in clinical medicine.[4] Particularly the covalent crosslinked network hydrogel with irregular and weak crosslinking points is easy to break and results in the structure's overall failure.[5] Physical crosslinking is formed through the physical bonds between different polymer chains. For example, ionically crosslinked gels are achieved by the interactions between charged polymers and counter ions. Previous studies show that higher mechanical strength might exist in hydrogels with physical crosslinking, providing new ideas for their application.[6,7] Though previous studies contributed a lot in synthesizing high-strength hydrogels or enhancing natural polymer hydrogels, the preparation of hydrogels combined with good biocompatibility and mechanical properties still faces many challenges.

Significant attention has been paid to exploring the characteristics and applications of GelMA in different research.[8] As mentioned in literature, GelMA is obtained by chemical modification and grafting of gelatin.[9] In fact, only 5% of the amino acid sequence of gelatin participates in the reaction. Therefore, the functional amino acid sequence of gelatin (such as RGD peptide sequence and MMP degradation sequence) is retained to the maximum extent. RGD can promote cell adhesion and growth,[10] and MMP is related to cell remodelling.[11] Specifically, the RGD amino acid sequence and MMP degradable sequence do not undergo methacrylate reaction, which means GelMA also has good biological activity, thus can promote cell adhesion and cell remodelling, and can be degraded by *in vivo* protease. Photo-crosslinking, performed in the presence of ultraviolet (UV) light and a chemical photoinitiator, is a type of chemical crosslinking which is safe and easy to conduct. The methacrylate substituent introduced in the GelMA structure enables UV photopolymerization and crosslinking reaction to prepare hydrogels. The polymerization conditions of GelMA are very mild. At room temperature, hydrogel can be formed in neutral pH, aqueous solution or biological liquid. Therefore, it has been widely used in the study of cell–material interaction and tissue engineering.

[a]*State Key Laboratory of Oral Diseases, National Clinical Research Center for Oral Diseases, West China Hospital of Stomatology, School of Chemical Engineering, Sichuan University, Chengdu, 610041, China*

[b]*Department of Neurosurgery, West China Hospital, Sichuan University, Chengdu, 610041, China*

[c]*State Key Laboratory of Polymer Materials Engineering, Sichuan University, Chengdu, 610065, China*

[d]*Department of Mechanical Engineering, The University of Hong Kong, Hong Kong, China*

† Electronic supplementary information (ESI) available. See DOI: https://doi.org/10.1039/d2ra06101e

‡ These authors contributed equally to this work.

Carrageenan is a natural soluble polysaccharide derived from various marine red algae.[12] It has a linear sulfated galactose skeleton. It is composed of α(1–3)-D-galactose-4 sulfation and β(1–4)-3, 6-dehydration-D-galactose alternately.[13] Among different kinds of carrageenan (such as κ, ι, λ), κ-carrageenan (KC) is more sensitive to the formation of K^+ ions. Each disaccharide unit at carbon 2 of the 1,3-linked galactose unit contains a sulfate group. The 4C1 conformation of 3,6-dehydrated-D-galactose unit allows a helical two-level structure, which is necessary to form gels.[14] According to the literature, the formation and melting of the KC are reversible.[15] The critical gel temperature and strength increase with the increase of KC concentration and cation content, making KC have great application space in synthesizing physical and chemical crosslinked double network (DN) hydrogels. In addition, the sol gel transition and gel sol transition of KC are thermally reversible. If KC is combined with GelMA and GelMA/KC DN hydrogel, DN hydrogels with better mechanical toughness and thermo reversibility are expected to be obtained. There is seldom report on synthesis and characterization of GelMA/KC DN hydrogel.

Given the unique advantages of hydrogel materials and their potential in biotherapeutics, the primary aim of the current study is to design and develop a GelMA/KC DN hydrogel with good mechanical strength and biocompatibility through dual-crosslinking mechanisms. Mechanical properties and dynamic rheological measurements were tested in the study. Furthermore, the activity of DN hydrogels loaded with BMSC was also measured. Cellular viability within hydrogel extracts, cell adhesion test, as well as the observation of cytoskeleton, will be evaluated as an assessment of their biocompatibility, potentiating their use in clinical applications.

2 Materials and methods

2.1 Materials

κ-Carrageenan (κ-CG), GelMA (Methacrylation degree of 60%), and I2959 were used as received from Aladdin Chemistry Co., Ltd. Fetal bovine serum (FBS), Dulbecco's modified Eagle's medium (DMEM), Cell counting kit-8 (CCK-8) were purchased from Jiangsu Keygen Biochemistry Co., Ltd. Triton X-100, FITC, DAPI were purchased by Beijing Solarbio Biochemistry Co., Ltd. HBMSC was purchased from Wuhan Procell Biochemistry Co., Ltd. Millipore deionized water was used in all the experiments.

2.2 Preparation of GelMA/KC DN hydrogel

The preparation process of GelMA/KC DN hydrogel by one-pot method is shown in Fig. 1. GelMA solid and KC powder with different masses were dissolved in deionized water. The concentration of GelMA was 10 wt% and 8 wt%, respectively, while the concentration of KC was 1 wt% and 0.5 wt%, respectively. Then, KCl (10% of the mass of KC) and I2959 (10% of GelMA mass) were added into the mixed solution of GelMA and KC, respectively. Attention should be paid to avoiding light after adding a photoinitiator. A uniform and transparent hot hybrid solution was obtained by magnetic stirring at 80 °C for 1 h. While hot, the solution was transferred to a round mold with a diameter of 20 mm and a thickness of 2 mm and a rectangular mold with length × width × height = 40 mm × 20 mm × 10 mm. Then, it was cooled at room temperature for 10 min to form the first physical crosslinked KC network. Then the molds were placed under UV lamp (365 nm, intensity 10 mW cm^{-2}) for photopolymerization of 1 min, and different concentrations of GelMA/KC DN hydrogels were obtained. After the preparation, the GelMA/KC DN hydrogels were removed from the mold and divided into different shapes according to the need for characterization experiments, mechanical properties tests and other experiments.

2.3 Material characterization

The prepared DN hydrogels were placed in a beaker and added liquid nitrogen to break them down at low temperatures. Then they were put into a freeze dryer to freeze them. The DN hydrogel was cut off after freeze-drying to expose the cross section. A scanning electron microscope was used to observe the microscopic morphology of the internal section. All fractures were sprayed with gold before they were observed. The different freeze-dried groups of hydrogels were grinded into agate mortar and powdered. The chemical composition and functional groups of GelMA/KC hydrogel were characterized by Fourier transform infrared spectroscopy. The pore size of each group of samples was measured by Image J software and analyzed. The equilibrium water content and water swelling ratio of GelMA/KC hydrogel were measured by gravimetric analysis. The fresh DN hydrogel samples were weighed by electronic balance and immersed in deionized water for 24 h respectively. When the hydrogel reaches the swelling equilibrium, the hydrogel is removed, and the surface water is removed to weigh the mass on the electronic balance. After that, the samples were dried in an oven at 60 °C, knowing that the hydrogel was completely dry and no longer had any mass loss. The formula for calculating the water content and swelling ratio of hydrogel is as follows (eqn (1) and (2)).

$$\text{Water content} = \frac{w_1 - w_2}{w_1} \times 100\% \quad (1)$$

$$\text{Swelling ratio} = \frac{w_1}{w_0} \times 100\% \quad (2)$$

w_0 is the of the weight prepared hydrogel. w_1 is the weight of the hydrogel after water swelling, and w_2 is the weight of the hydrogel after drying.

2.4 Mechanical property test and dynamic rheological measurement

The fresh DN hydrogel was cut into small cubes (10 mm × 10 mm × 8 mm), and the compression test was carried out by a universal testing machine. The specimens were compressed at a rate of 2 mm min^{-1} under a tensile load of 10 N at room temperature. The compression strain is estimated as h/h_0, where h is the compression height, and h_0 is the original height. The compressive strength and compression rate of hydrogel were studied. According to the slope of stress–strain curve, the Young's modulus of hydrogel can be determined.

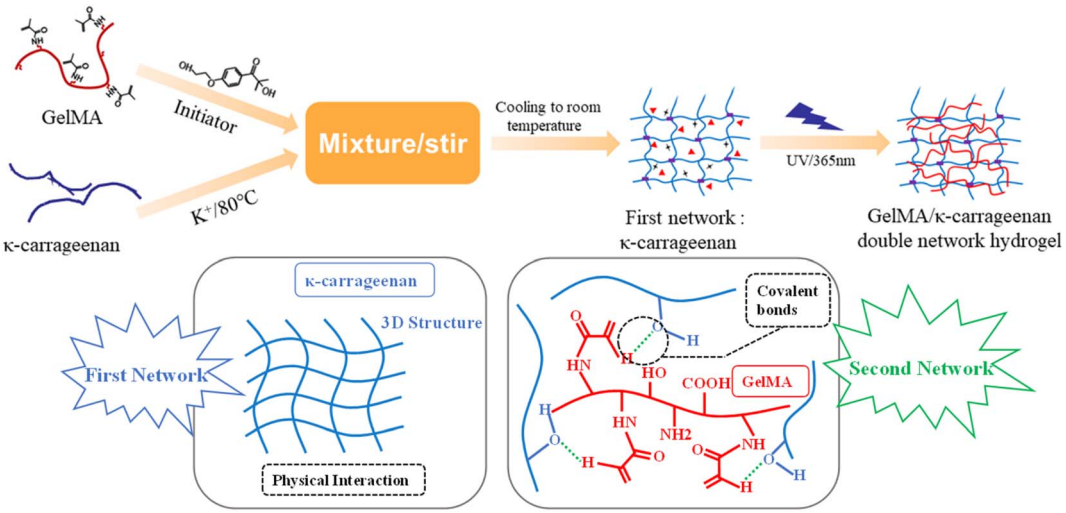

Fig. 1 Schematic diagram of the preparation of GelMA/κ-carrageenan double-network hydrogel by a "one-pot" tactic.

The rheological properties of KC hydrogel were tested by MCR302 rheometer and parallel plate clamp with a diameter of 25 mm. First, initialize the rheometer program, then install the fixture, select the appropriate program, adjust the parameters to 10 rad s^{-1}, shear range is 0.01–100%. After completing the preparation work, different groups of hydrogel samples were placed on the loading stage and measured in turn.

2.5 Culturing cells using hydrogel extracts

In this experiment, human bone marrow mesenchymal stem cells (hBMSCs) were selected to evaluate the biocompatibility of the materials in this chapter. And hBMSCs from passages 3-4 were used for experiments. The cells were grown in DMEM high glucose medium containing 10% FBS, 1% penicillin and streptomycin, and the medium was changed every two days. The cell culture flask containing cell suspension was placed in a constant temperature aseptic incubator with 5% carbon dioxide and 37 °C. When the cell coverage rate in the cell culture flask reached 90%, the fully grown cells were collected with trypsin, centrifuged with a standard medium, resuspended and diluted in a new culture dish. The containers and consumables used in the experiment were disposable sterile materials or sterilized by high pressure and were disinfected with 75% alcohol and ultraviolet before use. All operations should be carried out in sterile operation platform.

Before preparing hydrogel, the GelMA, KC, photoinitiator I2959 and KCl weighing 2 h were sterilized under an ultra-clean UV lamp. Then the sterilized GelMA and KC were dissolved in deionized water according to a specific concentration. The mixed solution was obtained by magnetic stirring for 1 h in the ultra-clean stage, adding photoinitiator I2959 and KCl. The above hybrid solution was transferred to the sterile cuboid mold (40 mm × 20 mm × 10 mm), and the hydrogel of KC network was obtained after cooling. Then the mold was placed in the ultraviolet lamp (wavelength: 365 nm, intensity: 10 mW cm^{-2}) for 1 min. After the reaction, aseptic GelMA/KC DN hydrogel with the same concentration was obtained.

After the aseptic hydrogel was prepared, GelMA/KC DN hydrogel extract was prepared according to ISO10993-12 standard. The hydrogel in each group was transferred to the centrifuge tube, and the DMEM medium without FBS was added at the ratio of 0.1 g mL^{-1}. The centrifuge tube was placed in a constant sterile incubator at 37 °C for 72 h. The extract of hydrogel was collected and filtered with 0.22 mm aseptic filter. The filtrated aseptic extract was placed in the 4 °C refrigerator for subsequent experiments.

HBMSCs were collected by trypsin and centrifuged. After redispersion in standard DMEM medium, hBMSCs were seeded into 48 well plate. The well plates were put back into a 37 °C incubator for 3 h. After all the cells were completely adhered to the wall, replace the culture medium in the plate with gel extract, then reenter the cell incubator for culture. The CCK-8 kit was used to investigate the proliferation of cells inoculated in hydrogel extracts, and CCK-8 activity was tested in the first, third and fifth days of culture, respectively. The cell supernatant was drawn from the well plate, and the cell metabolites in the well plate were washed with sterile PBS solution. Then 300 μL of standard DMEM medium containing 10% CCK-8 was added to the well plate, and the well plate was put into the cell incubator for 2–4 h. 100 μL supernatant was drawn from the incubated well plate to 96 well plate, and the absorbance of each group of solution was measured at 450 nm with a microplate reader. All operations were carried out in dark conditions. After the measurement, fresh 500 μL fresh gel extract was added to the original 48 well plate, and the orifice plate was placed in the cell incubator for further training.

2.6 Cell adhesion test

Cell adhesion was observed by SEM. HBMSCs cells were seeded into 24 well plate with sterile cell climbing plates placed in advance, and the density was 1 × 10^4 cells per mL. The plates

were incubated in a constant temperature sterile incubator at 37 °C for 3 h. After all cells were completely adhered to the wall, replace the water gel extract of Kong Banzhong's culture medium and reenter the cell incubator for 24 h. The cultured plates were taken out, the supernatant was removed, and the residual metabolites on the surface of the materials were cleaned with sterile PBS solution. Then, 4% paraformaldehyde was inhaled into each well to fix the cells on the surface of cell climbing plate. 500 μL paraformaldehyde was added into each well and fixed in a 4 °C refrigerator for 2 h. Each cell was dehydrated with different ethanol concentrations (v/v) for 15%, 50%, and 100%, respectively. Finally, the cells of each group were dried at the critical point and sprayed with gold on the surface for SEM observation.

2.7 Observation of cytoskeleton

To study the cytoskeleton of hBMSCs, hBMSCs were cultured in the material extract and observed by laser confocal microscope. The sterile cell climbing plate was put into 24 well plates in advance, and the cell suspension with a density of 1×10^4 cells per mL was inoculated in the well plate added with cell climbing plate. The well plate was incubated at 37 °C constant temperature sterile incubator for 3 h. After all cells were adhered entirely to the wall, replace the water gel extract of Kong Banzhong's culture medium and reenter the cell incubator for 24 h cultivation. Then the well plate was taken out, the cell culture supernatant was sucked out, and the cell slide was gently washed with sterile PBS buffer. Then, 4% paraformaldehyde solution and 0.1% Triton X-100 solution were added to each well and fixed for 30 min and permeabilized for 5 min in a refrigerator at 4 °C. After the permeabilization, 200 μL FITC labeled phalloidin dye was added to each well in a dark environment, and the cytoskeleton was stained for 30 min. Then 200 μL DAPI dye was added to stain the nuclei for 5 min. After all the staining steps were completed, the cells were placed on the stage, and the morphology of cytoskeleton was observed by laser confocal microscope.

2.8 Statistical analysis

Statistical analysis was performed by SPSS 19.0 software. ANOVA was used to determine homogeneity of variance between the groups. *T*-Tests were used to define significant differences among the groups. *P* values <0.05 were regarded as indicative of statistical significance. All results were expressed as means and standard deviations for at least three independent experiments.

3 Results and discussion

3.1 Formation and structure analysis

3.1.1 Fabrication of GelMA/KC DN hydrogels. It is well known that KC is a kind of negatively charged water-soluble biopolymer and contains one sulfate group per disaccharide unit. In general, the presence of K^+ facilitates the hardness of KC.[16,17] When temperature changes, KC can transform from coils to helices and aggregate double helices and then form a solid 3D network. These interactions promote the condensation of the double helices, as well as the generation of the first network. GelMA is a gelatin derivative containing methacrylamide groups. Under UV light exposure, GelMA molecules undergo photoinitiated radical polymerization, which leads to the introduction of methacrylamide groups to the main chain of KC. In this way, the covalently crosslinked second networks are formed.

We added initiator and K^+ into the mixture composed of GelMA and KC. After warming (80 °C), a sol–gel transition was achieved, followed by cooling to room temperature. Subsequently, UV light absorbed by the photoinitiator generates free radicals, which induce further polymerization and crosslinking. Thus, it is pretty easy to synthesize photo-cross-linkable DN hydrogels (Fig. 1), as already mentioned. Remarkably, after photoinitiator is added to the mixture, the mixture should be protected from light to maintain its stability or otherwise used immediately. Here, we employed solids with different weights to control the KC concentration (1 wt% and 0.5 wt%) and GelMA (10 wt% and 8 wt%). The prepared GelMA/KC DN hydrogels are parcellated into multiple shapes for further studies.

Fig. 2 presents photos of prepared hydrogels, which seem soft, yellow and moderately transparent. GelMA/KC DN hydrogels show higher turbidity, whereas GelMA hydrogel and KC hydrogel show higher transparency.

3.1.2 Effect of dual crosslinking on hydrogels microstructure. The mechanical performance of a material largely depends on its structure. GelMA hydrogels can be subjected to cryogenic treatments to generate porous scaffolds with controlled pore sizes and porosity.[18] So, we analyzed microstructures of the lyophilized KC, GelMA and GelMA/KC hydrogels using SEM (Fig. 3a–f). The structure of the porous scaffold is formed in all the hydrogels with GelMA. GelMA hydrogel presents a clear microscopic network formation with large and non-uniform pores. In contrast, KC hydrogel exhibits a layered structure, which leads to poor water absorption efficacy and low mechanical strength, rather than network formation. The GelMA/KC hydrogel shows distinctive morphologies because of

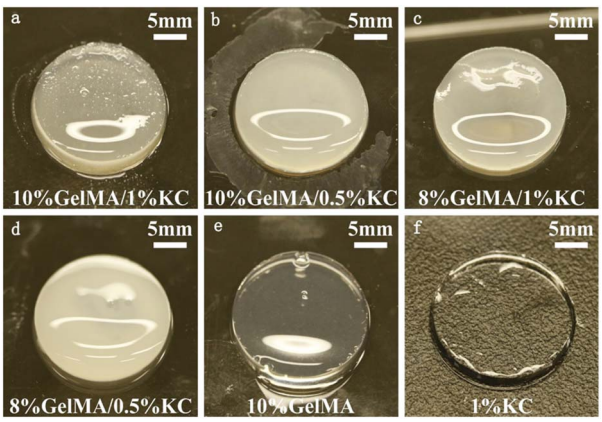

Fig. 2 Photos of the prepared hydrogels with (a) 10% GelMA/1% KC, (b) 10% GelMA/0.5% KC, (c) 8% GelMA/1% KC, (d) 8% GelMA/0.5% KC, (e) 10% GelMA, and (f) 1% KC hydrogels.

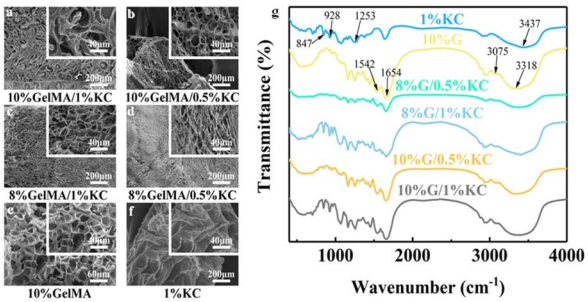

Fig. 3 (a–f) The morphology and microstructure, (g) FTIR spectra of different hydrogels.

the double network. Obviously, with decreasing amount of GelMA, the pore sizes of GelMA/KC hydrogels decrease, and the pore size distribution becomes tighter, proving the formation of a denser structure, as shown in Fig. 3a–f. Meanwhile, this dense porous structure is also accompanied by the increase in swelling ratio and equilibrium water content, as shown in Fig. S1.† It has been reported that hard hydrogel shows denser and less porous structures than soft hydrogel.[19] Consequently, a compact 3D structure is more conducive to enhancing the mechanical properties of GelMA/KC hydrogels. Furthermore, pore size distribution analysis of fabricated samples obtained by Image J also suggests the same results as SEM, as noted in Fig. S2.†

3.1.3 Formation and function group analysis of each synthesized hydrogel. FT-IR spectroscopy was performed on pure KC, GelMA hydrogels as well as the GelMA/KC hydrogels to examine their chemical composition and analyze the function groups (Fig. 3g). The characteristic peaks of KC at 1253 cm^{-1}, 928 cm^{-1}, 847 cm^{-1} and 859 cm^{-1} correspond to sulfate ester, 3, 6-anhydro-D-galactose and D-galactose-4-sulfate, respectively. A peak at 3437 cm^{-1} is related to the hydroxyl. The GelMA hydrogel exhibits apparent amide A at 3318 cm^{-1} and amide B at 3198 cm^{-1} for a stretching vibration of N–H. Amide I emerged from 1654 cm^{-1}, and amide II emerged from 1542 cm^{-1}. The former results in C–O stretching, while the latter results in N–H deformation of the primary amine, as well as C–N stretching vibration coupling. Comparatively, no new adsorption peak appeared from the FT-IR spectra of GelMA/KC hydrogels besides the characteristic peaks corresponding to KC and GelMA, demonstrating no new chemical bonds formed in the DN structure. In addition, there is a shift of glycosidic linkage in GelMA/KC hydrogels. The hydrogen bonding between the NH groups of GelMA and the OH groups of KC molecule could explain this. All the above results proved the presence of both materials and their successful blending.

3.2 Mechanical characterization of GelMA/KC double network hydrogels

The mechanical properties of each group of hydrogels were evaluated systematically. Photos of compression test are recorded in Fig. 4a, which confirms that ruptured materials present different morphology under the same type of stress, and the required stress is different. The stress–strain curves of hydrogel specimens are shown in Fig. 4b, in which GelMA/KC hydrogel gives high compressive strength. At the strain of 45%, compression strength of GelMA hydrogel (20 kPa) and κ-carrageenan (4 kPa) are both considerably lower than GelMA/KC hydrogel. This finding proves that the double network structure significantly improved the mechanical properties of hybrid hydrogels. Due to high concentration of GelMA, 10% GelMA/1% KC group and 10% GelMA/0.5% KC group reach the highest compressive strength of 130 kPa and 90 kPa, respectively. To the best of our knowledge, KC hydrogel formed *via* ionic crosslinking methods presents low stability in physiological settings.[8] On the contrary, the covalent bonds formed during crosslinking in photo-cross-linkable hydrogels render high stability to the polymer network.[20] These findings are consistent with our results. Fig. 4c shows Young's modulus of various materials, as well as the gap between pristine GelMA or KC hydrogel and GelMA/KC hydrogel. The achieved value of 10% GelMA/1% KC group (300 kPa), respectively, is 4 times of GelMA hydrogel (50 kPa) and 30 times of KC hydrogel (10 kPa), reflecting its better elasticity.

In the GelMA/KC hydrogels, the first network provides rigidity and fragility, while the second network provides elasticity and stretchability. Thus, mechanical properties of the material depend strongly on the KC, which generates the first network. In our study, although KC has lower compress strength and Young's modulus than GelMA hydrogel, physical crosslinks between KC molecules gave the hybrid hydrogel self-healing ability. When the material is unloaded, the physical bonds enable the hydrogels to reorganize and reconstruct, leading to the recovery of DN hydrogels. Many physically–chemically crosslinked DN hydrogels have been fabricated, such as agar/polyacrylamide,[21] alginate/polyacrylamide[22] and agar/polyvinyl alcohol[23] hydrogels, showing that GelMA/KC hydrogel designed by us has excellent potential for future research. From this study, we still cannot identify the trend of mechanical properties of the hybrid DN hydrogels with GelMA or KC concentration changing. Because it is impossible to judge the variation trend of a highly complex mixture with micro 3D structures only in 4 experimental groups. But if the mechanical property of the hydrogel is too high, the shearing stresses created by the hydrogel after implantation would hamper the new tissue ingrowth aside from the graft. Therefore, choosing the percentages of the various components of hybrid hydrogels in clinical use should rely on other properties, such as biocompatibility, instead of being overly concerned with having the best mechanical properties. However, it is still necessary to investigate because poor mechanical properties can greatly limit the applications in biomedical and engineering fields.

Rheological measurement was performed on an MCR302 rheometer with a parallel plate geometry of 25 mm in diameter to investigate elasticity and viscidity of the hydrogel samples. At a fixed temperature and shear rate, gradually increase the shear strain and then get the storage modulus (G') and loss modulus (G'') (Fig. 5a and b). The two curves reveal that for GelMA/KC hydrogel, G' and G'' are both higher than pristine hydrogels, suggesting that the generation of double networks is beneficial

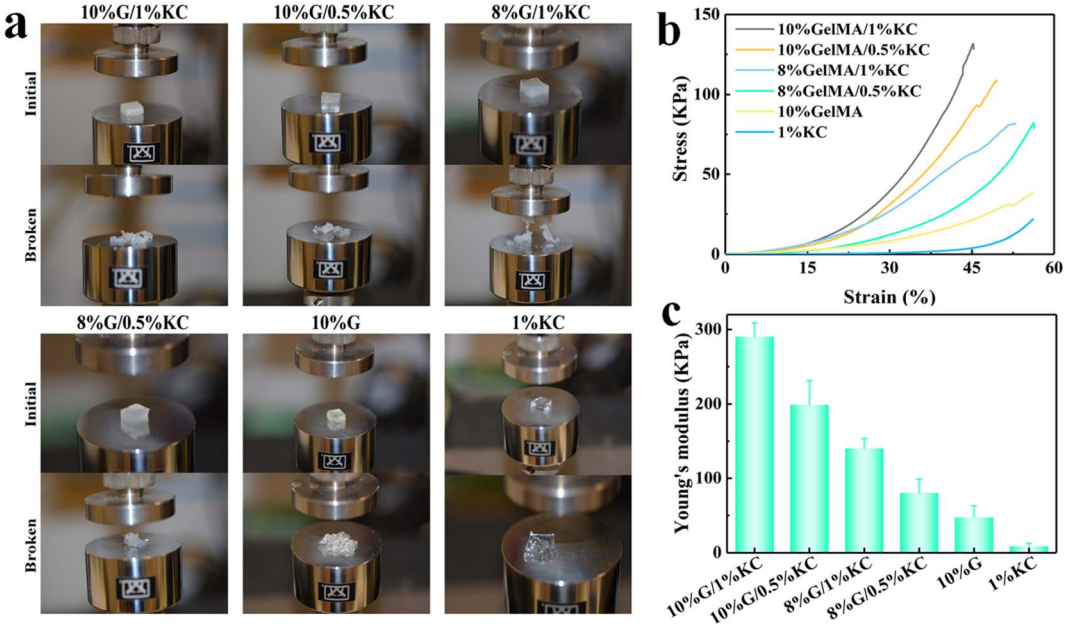

Fig. 4 (a) Comparative photos of different hydrogels before and after the compression tests, (b) the compressive stress–strain curves and (c) Young's modulus of the samples.

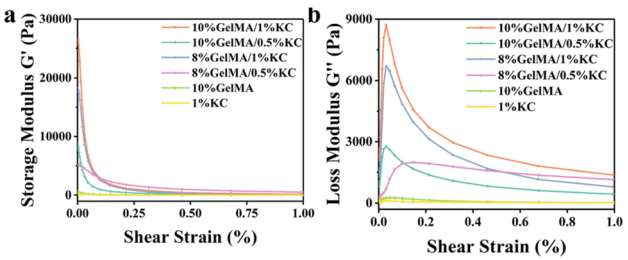

Fig. 5 (a) The storage modulus and (b) loss modulus of samples.

to enhance its mechanical strength, as well as slightly reducing its deformation. Moreover, the fact that results of 10% GelMA/1% KC group and 8% GelMA/1% KC group are higher than that of the other two groups might be ascribed to higher KC concentrations. This observed alteration could be attributed to the great influence of KC in changing mechanical properties of DN hydrogels.

3.3 Biocompatibility of GelMA/KC DN hydrogels

One of the primary requirements of any bioactive materials is biocompatibility. An ideal scaffold maintains cell viability, which exhibits excellent cell adhesion and proliferation.[24] As a collagen degradation product, GelMA is hypoimmunogenic and highly adaptable to cell attachment and growth, growth factor release and nutrient transport to surrounding cells.[25] Showing excellent biocompatibility, KC has been researched extensively. For example, KC can positively influence the adhesion and proliferation of human mesenchymal stem cells (hMSCs) and human pluripotent stem cells (hPSCs).[26] To evaluate biocompatibility of the samples, cells were seeded on the different extracts and cultured for 24 h. An inverted microscope further conducted cell morphology observation. HBMSCs in each sample shows a desirable extended morphology with antennas, confirming their suitable attachment and spreading, see Fig. 6a. At day 1, 3 and 5, cell proliferation was assessed using CCK-8 assay kit (Fig. 6b). Cell proliferation of DN hydrogels show drastic improvements compared with pristine GelMA or KC hydrogels. This finding suggests improved biocompatibility of the composite hydrogels. From most of the current works, we have noticed that physical properties of hydrogels are considered as essential factors for cell growth. It has been proven that tight and porous microstructure can increase the adhesion and reproduction of hMSCs.[27] We find that 8% GelMA/1% KC and 8% GelMA/0.5% KC groups present the maximum absorbance, indicating that the data may be associated with a tight porous structure. However, proportion of the two components in the GelMA/KC DN hydrogel that makes it achieve optimal cytocompatibility still needs to be further explored.

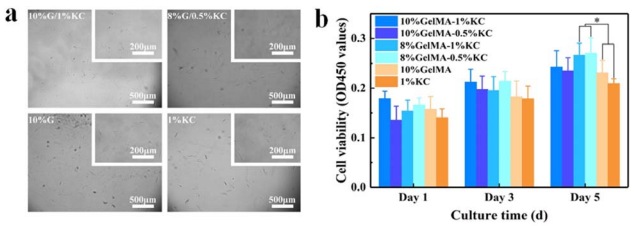

Fig. 6 (a) The optical microscope photos of hBMSCs cultured in the extracts of hydrogels, and (b) proliferation of hBMSCs after cultured 1, 3, and 5 days in the extracts of hydrogels ($n = 3$, $^*p < 0.05$).

Apart from cell morphology observation, we also tested hBMSCs for their adhesion using SEM (Fig. 7a). Only a small number of fusiform-shaped cells with incomplete spreading are attached to the cell climbing slices of pristine GelMA and KC groups. In contrast, hBMSCs grow adherently with significantly greater spreading area in GelMA/KC DN hydrogel groups. Research has established that cells adhere, remodel, and migrate through GelMA due to the presence of integrin-binding motifs and matrix metal proteinase sensitive groups.[10,11] In this study, cells in GelMA and DN hydrogel groups display more flat spreading morphologies than pristine KC group, indicating that GelMA hydrogel can generate the ideal environment for cell adhesion, remodeling, and migration. Additionally, the number of cells only embodied by SEM pictures may be inadequate compared to the pristine GelMA and KC samples. A greater number of hBMSCs adhere in GelMA/KC hydrogel samples. Especially 8% GelMA/1% KC group and 8% GelMA/0.5% KC group show the most extensive cell aggregation, in agreement with previous studies.

Biocompatibility of hydrogel samples was further assessed by cytoskeleton observation. Phalloidin and DAPI stained cells were examined after 24 hour's culture under a laser confocal microscopy to understand cell viability, morphology better and spreading (Fig. 7b). Based on the reported literature, nucleus is stained blue with DAPI, and the actin filaments are stained green with FITC targeted phalloidin under fluorescence. In our study, native spreading and protrusion extension morphologies are observed in GelMA/KC hydrogel samples. With enhanced cell adhesion, cells grown in the GelMA/KC hydrogel groups have more extended filopodia and spread better with visible mature F-actin fibers. On the contrary, in pristine hydrogel groups, just a small F-actin accumulation can be observed. Spindle-like shape cells are visible, inconsistent with the SEM images in Fig. 7b. Moreover, the number of cells in 8% GelMA/0.5% KC group(36) could recognize approximately 150% and 200% more than GelMA group(15) and KC group(12) respectively ($p < 0.05$). These results are clear indications supporting that GelMA/KC hydrogels are in favor of cell spreading and proliferation.

Cell metabolism in the materials is distinctly affected by the microenvironment, including molecular compositions and their spatial structure. As a gelatin derivative that retains RGD and matrix metalloproteinase amino acid sequences,[10,11] GelMA has inherent biocompatibility, including appropriate cell adhesion sites, and can be proteolytically degraded following implantation.[25] KC mimics biomimetic properties and resembles natural glycosaminoglycan structures.[28] Thus, the physical properties of hydrogels resemble the hydrated state of the native extracellular matrix (ECM). They exhibit high permeability to oxygen, nutrients and other soluble factors, which is vital for sustaining cellular metabolism. Furthermore, porous materials provide a microenvironment for cell growth, proliferation and the space for cell spreading.[29,30] That means biological behaviors are altered by the microstructure of scaffold. This is because mechanical performance of the material mainly depends on its structure, as mentioned before. For example,

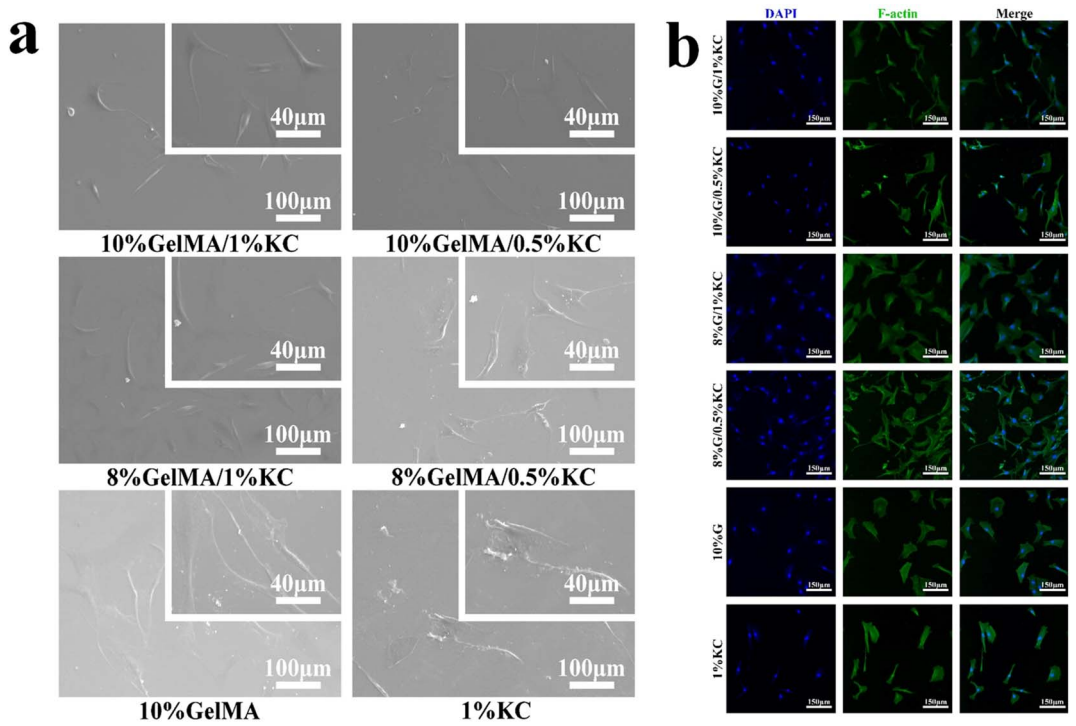

Fig. 7 (a) The morphology of hBMSCs adhesion by SEM images, cultured in the extracts of different samples for 24 h, (b) after culturing 24 h, CLMS images of hBMSCs stained by phalloidin and DAPI. Cell nucleus is stained by blue, and F-action was stained by the green (scale bar = 150 μm).

optimized bone remodeling happens when the scaffold elasticity matches or is slightly higher than that of the host bone.[31] In this research, the hybrid hydrogel has high elasticity modulus up to 300 kPa, providing mechanistic basis for cell growth and development. In addition, not all the pore chambers are suitable for tissue growth. Some pores are completely blocked, causing these areas unreachable to nutrition delivery and metabolite removal. Homogeneous and dense microstructure of DN hydrogel makes cellular metabolic in scaffold microenvironment more efficient. Recent studies have indicated that matrix stiffness plays a key role in stem cell proliferation and differentiation.[32] In agreement with our results, significantly elevated hBMSC proliferation were observed in stiffer DN hydrogels in comparison with traditional single-network hydrogels, demonstrating that DN hydrogel scaffolds with enhanced mechanic strength could also benefit hBMSC proliferation.

4 Conclusions

In summary, by using KC and GelMA materials, we have developed biodegradable and high-strength GelMA/KC DN hydrogels. The physically crosslinked first network makes the material brittle and stiff, whereas the covalently crosslinked second networks endow it with stretchable and elastic features. Moreover, the mechanical properties of the GelMA/KC hydrogels vary according to the concentration of each ingredient. DN hydrogel with higher GelMA concentration shows better physical property, indicating that the formation of the double network is beneficial to improve the mechanical properties of materials. Concerning biocompatibility, GelMA/KC hydrogels present better cytocompatibility, demonstrating that DN hydrogels are in favour of cell spreading and proliferation. Therefore, GelMA/KC DN hydrogel we designed in this study is a high-strength and biodegradable biomaterial expected to make essential contributions to the development of bone tissue engineering in the future.

Author contributions

Xueqi Gan: conceptualization, methodology, formal analysis, investigation, writing original draft, visualization. Chen Li: conceptualization, data curation, writing review & editing, funding acquisition, supervision. Jiyu Sun: formal analysis. Xidan Zhang: software. Min Zhou: investigation. Yi Deng: resources, funding acquisition, supervision. Anqi Xiao: validation, funding acquisition, supervision.

Conflicts of interest

There are no conflicts to declare.

Acknowledgements

We would like to thank Wen Tian and Yanping Huang from the Center of Engineering Experimental Teaching, School of Chemical Engineering, Sichuan University for the help with SEM and FT-IR measurements. This research was funded by the National Natural Science Foundation of China (81870802 and 81801306), Science and Technology Program of Sichuan Province (23ZDYF2069, 2019YFS0356, 2022YFS0320 and 2020YJ0297), the Natural Science Foundation of Sichuan Province (2022NSFSC0361), Chengdu International Science and Technology Cooperation Foundation (2020-GH03-00005-HZ, 2017-GH02-00025-HZ), State Key Laboratory of Polymer Materials Engineering (Grant No. sklpme2019-2-05), Young Elite Scientist Sponsorship Program by CAST, Sichuan University-Luzhou City Special Funding for Strategic Cooperation (Grant No. 2020CDLZ-5) as well as Hong Kong Scholar.

References

1 A. Yaghoubi, A. Ramazani and H. Ghasemzadeh, *RSC Adv.*, 2021, **11**, 39095–39107.
2 D. Das and S. Pal, *RSC Adv.*, 2015, **5**, 25014–25050.
3 W. X. Waresindo, H. R. Luthfianti, D. Edikresnha, T. Suciati, F. A. Noor and K. Khairurrijal, *RSC Adv.*, 2021, **11**, 30156–30171.
4 Y. Huang, L. Xiao, J. Zhou, X. Li, J. Liu and M. Zeng, *J. Mater. Sci.*, 2020, **55**, 14690–14701.
5 J. P. Gong, Y. Katsuyama, T. Kurokawa and Y. Osada, *Adv. Mater.*, 2003, **15**, 1155–1158.
6 A. Mandal, J. R. Clegg, A. C. Anselmo and S. Mitragotri, *Bioeng. Transl. Med.*, 2020, **5**, e10158.
7 S. Cuenot, P. Gelebart, C. Sinquin, S. Colliec-Jouault and A. Zykwinska, *J. Mech. Behav. Biomed. Mater.*, 2022, **133**, 105343.
8 H. C. Yu, C. Y. Li, M. Du, Y. Song, Z. L. Wu and Q. Zheng, *Macromolecules*, 2019, **52**, 629–638.
9 A. Safaei-Yaraziz, S. Akbari-Birgani and N. Nikfarjam, *RSC Adv.*, 2021, **11**, 22544–22555.
10 C. Puckert, E. Tomaskovic-Crook, S. Gambhir, G. G. Wallace, J. M. Crook and M. J. Higgins, *Acta Biomater.*, 2020, **106**, 156–169.
11 A. E. Gilchrist, S. Lee, Y. Hu and B. A. C. Harley, *Adv. Healthcare Mater.*, 2019, **8**, e1900751.
12 I. M. Yermak, V. I. Gorbach, I. A. Karnakov, V. N. Davydova, E. A. Pimenova, C. Chistyulin Dcapital A, V. V. Isakov and V. P. Glazunov, *Carbohydr. Polym.*, 2021, **272**, 118479.
13 R. Rupert, K. F. Rodrigues, V. Y. Thien and W. T. L. Yong, *Front. Plant Sci.*, 2022, **13**, 859635.
14 Y. Deng, M. Huang, D. Sun, Y. Hou, Y. Li, T. Dong, X. Wang, L. Zhang and W. Yang, *ACS Appl. Mater. Interfaces*, 2018, **10**, 37544–37554.
15 Y. Wang, C. Yuan, Y. Liu, D. Xu and B. Cui, *Food Hydrocolloids*, 2019, **90**, 276–284.
16 S. R. Derkach, N. G. Voron'ko, Y. A. Kuchina, D. S. Kolotova, A. M. Gordeeva, D. A. Faizullin, Y. A. Gusev, Y. F. Zuev and O. N. Makshakova, *Carbohydr. Polym.*, 2018, **197**, 66–74.
17 H. Chen, D. Wu, W. Ma, C. Wu, Y. Tian, S. Wang and M. Du, *Food Hydrocolloids*, 2021, **119**, 106841.
18 E. Jamshidifar, M. Esfandyari-Manesh, H. Motasadizadeh, S. Naderizadeh, A. Yourdkhani, N. Samadi and R. Dinarvand, *J. Mater. Sci.*, 2022, **57**, 13603–13619.

19 F. Souza Almeida, K. C. Guedes Silva, A. Matias Navarrete de Toledo and A. C. Kawazoe Sato, *J. Food Sci. Technol.*, 2021, **58**, 302–310.
20 I. Silvestro, R. Sergi, A. Scotto d'Abusco, A. Mariano, A. Martinelli, A. Piozzi and I. Francolini, *Carbohydr. Polym.*, 2021, **267**, 118156.
21 F. Ding, W. Tang, L. Fu, R. Zhang, G. Wang, Z. Han, R. Wu, Y. Dong and X. Zou, *Polymer*, 2022, **238**, 124387.
22 J. Yi, K. T. Nguyen, W. Wang, W. Yang, M. Pan, E. Lou, P. W. Major, L. H. Le and H. Zeng, *J. Colloid Interface Sci.*, 2020, **578**, 598–607.
23 R. Wang, N. Li, B. Jiang, J. Li, W. Hong and T. Jiao, *Colloids Surf., A*, 2021, **615**, 126270.
24 S. Naahidi, M. Jafari, M. Logan, Y. Wang, Y. Yuan, H. Bae, B. Dixon and P. Chen, *Biotechnol. Adv.*, 2017, **35**, 530–544.
25 X. Bi, P. Maturavongsadit, Y. Tan, M. Watts, E. Bi, Z. Kegley, S. Morton, L. Lu, Q. Wang and A. Liang, *Bio-Med. Mater. Eng.*, 2019, **30**, 111–123.
26 S. Xiao, T. Zhao, J. Wang, C. Wang, J. Du, L. Ying, J. Lin, C. Zhang, W. Hu, L. Wang and K. Xu, *Stem Cell Rev. Rep.*, 2019, **15**, 664–679.
27 S. Vignesh, A. Gopalakrishnan, M. R. Poorna, S. V. Nair, R. Jayakumar and U. Mony, *Int. J. Biol. Macromol.*, 2018, **112**, 737–744.
28 M. Spreda, N. Hauptmann, V. Lehner, C. Biehl, K. Liefeith and K. S. Lips, *Molecules*, 2021, **26**, 6258.
29 E. Yalcin, G. Kara, E. Celik, F. A. Pinarli, G. Saylam, C. Sucularli, S. Ozturk, E. Yilmaz, O. Bayir, M. H. Korkmaz and E. B. Denkbas, *Prep. Biochem. Biotechnol.*, 2019, **49**, 659–670.
30 I. Fernández-Cervantes, M. A. Morales, R. Agustín-Serrano, M. Cardenas-García, P. V. Pérez-Luna, B. L. Arroyo-Reyes and A. Maldonado-García, *J. Mater. Sci.*, 2019, **54**, 9478–9496.
31 N. Abbasi, S. Hamlet, R. M. Love and N.-T. Nguyen, *J. Sci.: Adv. Mater. Devices*, 2020, **5**, 1–9.
32 M. Sun, G. Chi, P. Li, S. Lv, J. Xu, Z. Xu, Y. Xia, Y. Tan, J. Xu, L. Li and Y. Li, *Int. J. Med. Sci.*, 2018, **15**, 257–268.